Advanced GNSS Algorithms for Safe Autonomous Vehicles

E. Domínguez Tijero, E. Carbonell Pons, J.D. Calle Calle, L. Martínez Fernández, P.F. Navarro Madrid, C. Moriana Varo, M. Azaola Sáenz, *GMV, Spain*

BIOGRAPHY

Enrique Domínguez Tijero received a M.Sc. degree in Telecommunications Engineering in 2000 and a Master in Space Technologies in 2009, both from the Polytechnic University of Madrid. He joined GMV in 2000 working first in the development of EGNOS and Galileo and since 2009 in GNSS software receivers, multi-sensor fusion algorithms and integrity algorithms.

Enrique Carbonell Pons has an MSc degree in Aerospace Engineering from the Universidad Politécnica de Valencia (Spain) and Cranfield University (UK). He joined GMV in 2014 and he has been working in the GNSS business unit designing and developing algorithms and applications. He has emphasized his career on Precise Point Positioning (PPP) and Positioning Integrity algorithms. He is currently leading PPP activities both in the ESCAPE project for GSA, and the Satellite-Based Positioning Augmentation Demonstrator for Geoscience Australia.

J. David Calle holds a Master of Science in Computer Engineering from the University of Salamanca. He joined GMV in 2008 and he has been working in the GNSS business unit involved in the design and development of GNSS algorithms, applications and systems. He is currently Head of GNSS Services Section coordinating the activities related to the Galileo Commercial Service, Open Service Authentication and High Accuracy provision services.

L. Martínez Fernández holds a Degree in Aerospace Engineering from the Polytechnic University of Valencia, specialty in Aero-navigation, and an MSc in Aeronautical Engineering from Polytechnic University of Catalonia, specialty in Space. She joined the GMV as a GNSS engineer working in activities related with magicGNSS, more concretely in precise orbit determination, precise positioning and integrity algorithms.

Pedro F. Navarro Madrid has a Master of Science in Mathematics from the University of Murcia (Spain) and Postgraduate studies in Theoretical Physics at the University of Valencia (Spain). He has worked at GMV since 2002 as an engineer in the development of Galileo and later in R&D activities covering both the ground and user segments.

Carlos Moriana Varo has a Master of Science in Telecommunications Engineering from the Carlos III University and a Master in Space Technology from the Technical University of Madrid. He has worked at GMV since 2009 as engineer in several GNSS projects focused on sensor fusion and navigation and integrity algorithms applied to urban environments.

Miguel Azaola Sáenz has a Master of Science in Mathematics from the University Complutense of Madrid and a Ph.D. in Mathematics (in the field of Geometry and Topology) from the University of Cantabria (at Santander, Spain). He has worked at GMV since 2001 as an engineer in several GNSS projects related to both the ground and user segments. Since 2005 he has been involved in user segment R&D activities at engineering and management levels.

ABSTRACT

The main concern of autonomous driving (AD) is the safety of human beings, both inside and outside the vehicle. Safety depends on a wide variety of complex factors such as vehicle speed, weather, state of the road, complexity of the environment (surrounding vehicles, pedestrians or obstacles), or situational awareness, among others. In order to cope with these factors, different sensors are placed in the vehicle to measure dozens of parameters (absolute speed, distance to surrounding vehicles and pedestrians, relative speed, absolute position, distance to next crossing, etc.). Accurate knowledge of these and other parameters is a key to safety, but even more important is to ensure their reliability. Such guarantee on reliability is what the aviation community refers to as integrity. The implementation of an integrity layer is crucial since in safety-critical applications it can be more important to know whether information is reliable than the precise information itself.

Attempts to rely positioning integrity of land users upon the use of Satellite Based Augmentation Systems (SBAS) only have revealed major shortages, given that SBAS integrity has been conceived for use in open sky and clean operation scenarios as it is the case of aviation users. As a result, a lot of effort is being devoted to the investigation of autonomous techniques for determining the integrity of the navigation solution taking into account the local effects on GNSS signals in harsh environmental conditions.

GMV has been working for a decade in developing GNSS-based navigation systems for automotive applications

where integrity and accuracy are top-priority requirements. As a result, GMV has developed navigation technologies of very high accuracy and proven integrity which can combine GNSS with a wide variety of other sensors both from the vehicle (accessed through CAN bus) and external to it (low-cost inertial sensors have been successfully hybridised with GNSS in aftermarket integrity-enabled solutions).

The purpose of this paper is to present the performances achieved with GMV navigation and integrity technologies, which are an input to automotive applications like in ESCAPE project ([1]), where the GNSS-based systems are essential and where the GMV navigation and integrity technologies will be combined with vehicle sensors and camera measurements to provide an accurate and reliable solution.

ESCAPE (European Safety Critical Applications Positioning Engine) is a project co-funded by the European GNSS Agency (GSA) under the European Union's Fundamental Elements research and development programme. It started on October 2016 with duration of 3 years and with the main objective of developing a localisation system that provides the vehicle pose estimates to be employed in safety critical applications like Autonomous Driving (AD) or Advanced Driving Assistance Systems (ADAS). The project is led by the Spanish company FICOSA in collaboration with partners from across Europe: Renault and IFSSTAR from France, STMicroelectronics and Instituto Superiore Mario Boella from Italy and GMV from Spain. ESCAPE will enable a high-grade of data fusion with different vehicle sensors and the exploitation of key technological differentiators such as the Precise Point Positioning service (PPP), the potential use of the Galileo ionospheric model and the provision of an integrity layer to assess the degree of trust one can associate to the position information provided by the device.

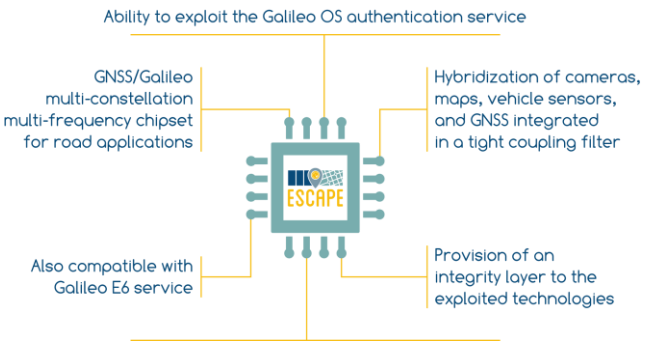

Figure 1 ESCAPE Core Features

INTRODUCTION

The current paper showcases the latest accuracy and integrity results obtained by GMV in automotive applications with its advanced GNSS processing technologies. Different techniques are covered such as hybrid GNSS/INS navigation solutions, PPP and, very in particular, positioning integrity in ITS environment based on KIPL technology, which is based on monitoring local effects for positioning error bounding computation. All of these technologies have been developed by GMV thanks to an ambitious R&D programme that started 10 years ago. These latest obtained performances are an input to the ESCAPE project and one of its key assets. Throughout this paper, the following techniques will be presented:

- Standard Hybrid GNSS/INS Navigation + KIPL: Navigation solution adapted for road applications in urban environments which combines multi-constellation GNSS and INS measurements. The integrity layer is undertaken by the KIPL algorithm, being able to provide tight integrity bounds in all kinds of environments for virtually any desired confidence level. The results of a test campaign carried out in the city of Madrid (Spain) are presented, paying attention to the levels of integrity achieved as well as to the size of the obtained integrity bounds.

- PPP navigation using mass-market receivers + Integrity bound computation (KIPL). The PPP algorithm has been optimised to operate with mass-market GNSS receivers –focusing on automotive-type receivers- , allowing sub-decimetric level positioning using low-quality measurements gathered by these chipsets. The complexity of dealing with low-end GNSS equipment for PPP (single frequency measurements, high code-phase noise, low multipath rejection at the antenna, etc) has been addressed in GMV's real-time PPP client as part of recent R&D activities. In addition, the KIPL algorithm has been adapted to these receivers in order to produce tight integrity-based Protection Levels (PLs) to the positioning error based on a mathematically sound algorithm tailored to PPP. The results of an experimentation campaign with mass-market PPP + KIPL algorithms in static, kinematic (urban, peri-urban and open sky) and convergence scenarios will be presented in this paper.

Besides, the results presented in this paper will help any autonomous or assisted vehicle application to be aware of the accuracy and integrity peformances that can be achieved by cutting edge advanced GNSS technologies in challenging environments and how they can be employed to enhance safety.

The following section will provide a brief description of the KIPL integrity algorithm and the following two sections will present the accuracy and integrity performances achieved by GMV techniques.

KIPL INTEGRITY ALGORITHM

The KIPL (Kalman Integrated Protection Level) is a technique to compute Protection Levels (PLs) for the

navigation solution obtained from a Kalman filter so it can be applied to both Kalman filters: the hybrid GNSS/INS and the PPP. KIPL is partly a development of the ideas of IBPL (Isotropy-Based Protection Level), which applies for least-squares solutions based on the isotropy concept ([2] and [3]), extended to filtered solutions (see KIPL details in [4] and [5] and in patents [6] and [7]). KIPL is also employed in the navigation and integrity (PVT+I) solution of the SRX GMV software receiver product [8].

The main ingredients of the KIPL method are:

- a family of probability distributions that model the different contributions to the navigation error;
- a procedure to dynamically compute and update probability distributions associated to each error source (e.g. measurement errors);
- a step to compute a PL associated to a given Integrity Risk from the probability distributions.

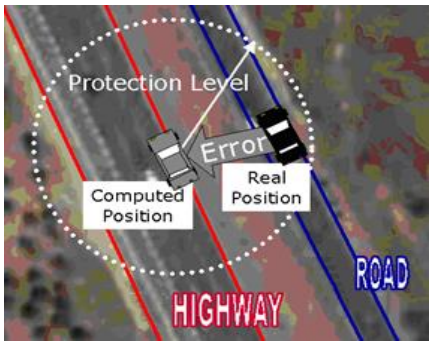

Figure 2 Horizontal Protection Level Concept

The family of probability distributions chosen to characterize the different error contributions is that of multivariate t-distributions. They provide an estimation of the errors covariance but also an indicator of the confidence that this assessment deserves. This family is parameterized by a scalar, which is usually known as the number of degrees of freedom, and a covariance matrix, which gives an estimation of the size of the errors.

The t-distribution is heavy tailed and it provides a more realistic representation of the measurement and navigation errors than the normal distribution.

The KIPL method introduces a probability distribution for each of the relevant error sources: measurement errors (code, carrier-phase, Doppler), propagation errors, etc... Each distribution is processed and updated separately and provides a contribution to the total Protection Level. There are two main components in this process:

- Characterization of the measurements errors, which is dynamically monitored as the level of noise may be quickly changing as a result of the environment (e.g. user in an urban area). This characterization allows to estimate an error distribution of the measurement errors at each epoch.
- Update of the different errors distributions as the Kalman filter updates its solution. This computation is based on what the estimation module actually does to derive the solution. Hence, the integrity method requires a detailed knowledge of the Kalman filter update and propagation operations.

The driving principle behind the construction of these distributions is that new errors are introduced in the solution at each epoch, while the errors in the previous solution are also carried over to the new solution. In order to take these factors into account, the integrity algorithm employs the Kalman filter matrices which provide the following information from the estimation step:

- Dependence of the updated solution on the measurements at current epoch
- Dependence of the updated solution on the previous solution
- Propagation equation and associated covariance matrix (process noise)

Finally, once the t-distribution for the solution errors is known, it is straightforward to obtain the PL associated to any given Integrity Risk α, or confidence level $(1-\alpha)$. As the method is based on modelling the distribution of errors, rather than putting fairly conservative limits, it provides tight integrity bounds and is suited both for high and low confidence levels.

$$\boldsymbol{P(\varepsilon > PL) < \alpha}$$

where ε is the error that we wish to bound.

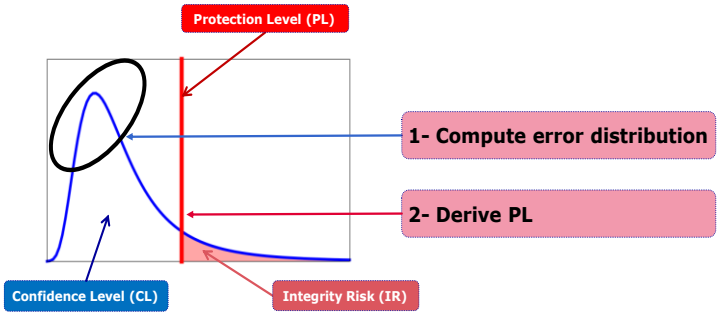

Figure 3 PL computed from error distribution

KIPL method is a reliability bound computation algorithm that offers integrity to any Kalman navigation solution.

STANDARD HYBRID GNSS/INS NAVIGATION (SPP) + KIPL

This technology is based on a Kalman filter that employs multi-constellation GNSS along with INS measurements, if available, to compute position and velocity combined with a Fault Detection and Exclusion (FDE) mechanism, to avoid using measurements with high errors. It also employs the KIPL algorithm to compute the PLs, thus providing an integrity layer to the navigation solution.

This section provides the accuracy and integrity results obtained in two different extensive field campaigns carried out in Madrid and London as part of a GMV internal research project ([4]) and the IGNSSRX EC project ([9])

respectively. A brief description of the field campaigns will be provided before showing the obtained results.

Madrid

The hybrid Kalman filter and KIPL integrity method have been implemented in an on-board unit (OBU) based on the ST Microelectronics' Teseo-II low-cost GPS/GLONASS chipset. It includes an inertial measurement unit (IMU) consisting of a 3-axis accelerometer and a 3-axis gyro. The navigation module is based on a Kalman filter that processes the GNSS raw data provided by Teseo-II and the inertial data from the IMU. The hybridizing of GNSS with inertial sensors is made through a tight coupling scheme. The filter incorporates an efficient mechanism for fault detection and exclusion (FDE), very important in harsh environments as urban canyons to exclude degraded measurements, especially those affected by NLoS (Non Line of Sight). The integrity module runs in parallel with the Kalman filter and computes Protection Levels based on the intermediate matrices and residuals obtained in the navigation module. See [4] for further details.

The field campaign was conducted comprising several hours of data, gathered along a track which includes highway and suburban legs, but most of which corresponds to a deep urban canyon area in Madrid downtown known as Salamanca district. Figure 4 shows the test route as a red track which was covered several times.

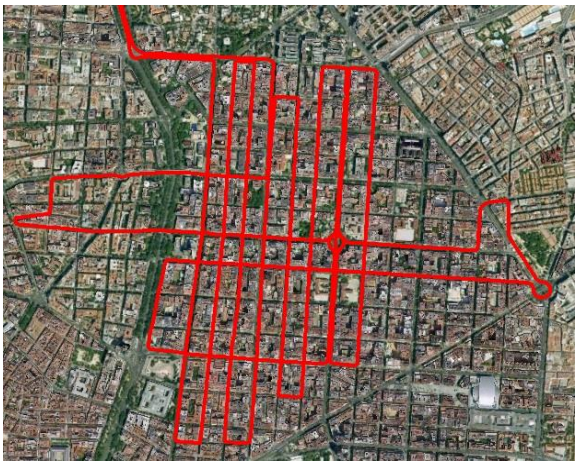

Figure 4 Madrid – Urban field campaign track (downtown)

In order to carry out the field campaign the test vehicle was equipped with a high performance reference positioning system based on a NovAtel SPAN-SE receiver and a (tactical-grade) iMAR FSAS IMU.

The samples gathered on different days have been put together to compute the relevant statistics. In total, there are more than 150,000 samples (42 h). However, since the performance strongly depends on the characteristics of the environment, the samples have been classified in three groups reflecting different surroundings:

- Open Sky
- Inter-urban
- Urban canyon

London

In the London field campaign the vehicle was equipped with the TRITON L1 Front-End ([10]) and the GPS and GLONASS measurements were generated with the SRX software receiver [8] and processed with the GMV navigation Kalman filter and KIPL integrity method (but in this campaign it was not hybridized with IMU measurements). The test vehicle was also equipped with a high performance reference positioning system based on a NovAtel GPS&GLONASS L1/L2 with SPAN-CPT IMU and wheel sensor. See [9] for further details.

The London field campaign covered motorway and urban environments (urban including tunnels and urban canyons), with a total of 110 hours of usable data, 40 hours in motorway and 70 hours in urban environments.

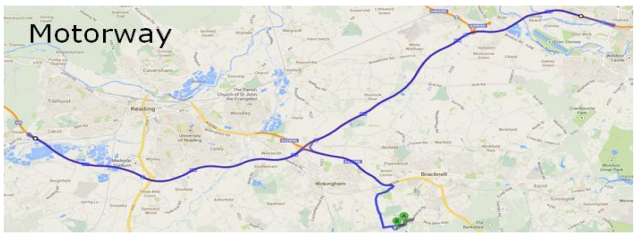

Figure 5 London - Vehicle Data Collection: Motorway route

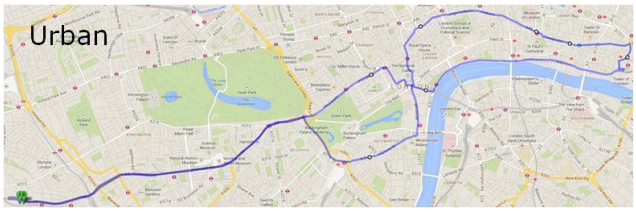

Figure 6- London - Vehicle Data Collection: Urban route

The following sub-sections will report the results, in terms of accuracy, availability and integrity, obtained in the both field campaigns for the different environments.

But first, it is important to highlight the differences between the London and Madrid campaigns. While the characteristics of the open-sky/motorway environment in both campaigns were very similar, the urban environments had several differences. On the one hand, the urban canyons present in the London field tests were at some parts of the route narrower than in the Madrid field tests which reduces the visibility and affects the performances at higher percentiles. Therefore, the London results will be worse than the Madrid ones at the higher percentiles because of the slightly harsher urban environment. On the other hand, the Madrid field tests passed through tunnels in the inter-urban environment while there was no tunnel within the urban route, but in the London campaign there were tunnels placed in the urban environment. The presence of tunnels will have a greater impact on the error of the navigation algorithm running only with GNSS measurements (without IMU), degrading its performance for the highest percentile because only a few epochs are affected by the tunnels compared to the total ones.

Accuracy

Table 1 contains the Horizontal Positioning Error (HPE) at different percentiles for the different campaigns and types of environment: Open Sky, Inter-urban and Urban.

The differences between the accuracy performances obtained in London and Madrid campaigns are as expected, in line with the mentioned differences between both campaigns with respect to the tunnels and urban conditions. The best accuracy is obtained in open sky conditions, where the size of the horizontal error is typically a few meters, whereas in urban environment the error reaches 10-15 m around 10% of the epochs. The use of inertial sensors improves the performances in all the cases. The results are good for a low-cost receiver given the harshness of the environment.

Accuracy - HPE [m]						
Env.	Campaign	Meas	Percentile [%]			
			50	90	95	99
Open-Sky (Motorway)	London	GNSS-only	2.0	4.4	5.8	9.6
	Madrid	GNSS-only	2.3	4.3	5.2	8.2
		GNSS+IMU	2.2	3.8	4.5	6.0
Inter-Urban	Madrid	GNSS-only	2.7	7.5	10.2	17.6
		GNSS+IMU	2.6	6.5	8.7	14.9
Urban	London	GNSS-only	4.9	16.2	22.2	81.8
	Madrid	GNSS-only	4.9	11.0	14.1	21.7
		GNSS+IMU	4.4	9.3	11.7	18.3

Table 1: Accuracy - HPE [m] representative percentiles

Size of the HPLs (Availability)

Taking into account that the size of the computed Horizontal Protection Level (HPL) will be checked before employing the computed solution, the availability of the computed solution will be driven by the size of the computed HPL.

Table 2 shows the statistical behavior of the horizontal error bounds or HPLs as computed for Target Integrity Risk (TIR) values of 10^{-4}. The table contains the representative percentiles for the different campaigns and GNSS-only and GNSS+IMU processing types.

Availability - HPL [m] for TIR=1E-4						
Env.	Campaign	Meas	Percentile [%]			
			50	90	95	99
Open-Sky (Motorway)	London	GNSS-only	13.5	29.0	32.8	48.8
	Madrid	GNSS-only	26.3	42.0	48.5	67.6
		GNSS+IMU	21.1	29.4	32.2	36.8
Inter-Urban	Madrid	GNSS-only	31.9	52.7	67.8	136.9
		GNSS+IMU	24.9	36.1	42.4	129.8
Urban	London	GNSS-only	41.8	64.4	77.6	143.7
	Madrid	GNSS-only	36.6	53.9	62.2	91.2
		GNSS+IMU	28.6	39.5	45.6	69.6

Table 2: Availability - HPL [m] representative percentiles for TIR=1E-4

The differences between the availability performances obtained in London and Madrid campaigns are as expected, in line with the mentioned differences between both campaigns with respect to the tunnels and urban conditions. The slightly harsher urban conditions in the London campaign lead to slightly higher HPLs when compared with the ones obtained in the Madrid campaign. Besides, the tunnel present in the Madrid inter-urban route and the tunnels present in the London urban route degrade the 99th percentiles (when going through a tunnel in GNSS-only mode the Kalman filter is not receiving any measurement so the confidence on the provided solution will decrease making the PLs to increase).

There is a clear enhancement of availability when using IMU data, even more visible than the improvement obtained in accuracy. This hints that the coupling with the inertial sensors brings a benefit to integrity not only due to the better accuracy obtained, but also by allowing a better assessment of the measurements quality.

If we compare with the accuracy performances, it appears that the PL size fits very well with the size of the errors. Only as an example, Protection Levels for a Target Integrity Risk of 10^{-4} in the Madrid highly demanding urban scenario is smaller than 40 meters 90% of the time (GNSS+IMU), whereas the corresponding accuracy percentile at 90% is around 10m. Besides, it should be noted that, although the complete performances for all the TIR values are not provided in this paper, for TIR=0.05 the PLs are below 18m 90% of the time, demonstrating a very good adjustment of the algorithm to the real statistics.

Integrity

As expected, the PLs computed by the KIPL algorithm show a clear correlation with the errors obtained at each moment, automatically reacting to the increase of the positioning errors and thus, to changes in the environment.

	$\frac{Nº Failures}{Nº Samples} / TIR$			
TIR	Madrid		London	
	GNSS-only	GNSS+IMU	GNSS-only	
			Motorway	Urban
1E-1	0.25	0.38	-	-
5E-2	0.26	0.33	-	-
1E-2	0.31	0.46	-	-
1E-3	0.66	0.78	0.05	0.82
1E-4	0.46	0.18	0	0.99
1E-5	0	0	-	-
1E-6	0	0	-	-
1E-7	0	0	-	-

Table 3: Integrity - Normalized Integrity Risk (Measured IR/TIR)

In order to obtain meaningful failure rate figures, especially for high confidence levels, it was necessary to accumulate as large a number of samples as possible. Table 3 shows the results (separating by type of solution) obtained using all samples acquired during the campaign.

The number of samples is above 150,000 in the Madrid campaign and around 400,000 in the London campaign. The table columns contain the experimental rate of integrity failures, compared to the target integrity risk (TIR). This metric is computed by taking, for each target integrity risk, the overall fraction of epochs where the horizontal error is above the PL and normalizing by the corresponding TIR. Hence, the integrity algorithm complies with the TIR whenever the metric is equal to or below 1.

As the table shows, the integrity failure rate values obtained are always below the Target Integrity Risk, which means that the error bounds are even safer than intended, or in other words, that the integrity risk requirements are always satisfied. In addition, the rates are similar for the different target integrity risks for which the sample size is appropriate. That is, KIPL is not restricted to a concrete value of TIR.

A compact way of visualizing accuracy and integrity performances all at once is by means of so-called Stanford diagrams. Each point in the Stanford plot represents one sample whose abscise is the (horizontal) position error and whose ordinate is its associated error bound as provided in real time by the integrity algorithm. So accuracy and error bound size performances can be visualized by looking at abscise and ordinate values, respectively, of the points in the plot. Integrity failure events, understood as failures of the error bound to cover the corresponding position error, are represented by points below the diagonal. The Stanford diagrams have been computed for the GNSS-only and GNSS+IMU solutions, considering the set of error bounds computed for a Target Integrity Risk of 10^{-4}.

As expected, the dispersion is higher in the urban canyon environment and lower in open-sky/motorway conditions. In the same way, the use of IMU data allows smaller PLs. All in all, these diagrams prove that the PLs computed by the KIPL algorithm provides a means to offer integrity to a Kalman solution, even in difficult conditions.

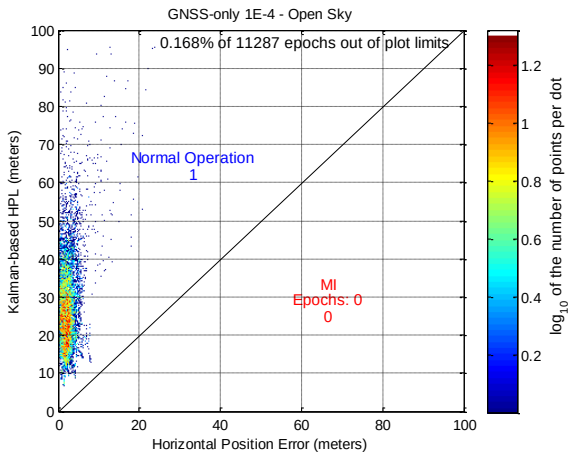

Figure 7 Madrid - Stanford diagram, GNSS-only, Open-Sky (TIR =1E-4)

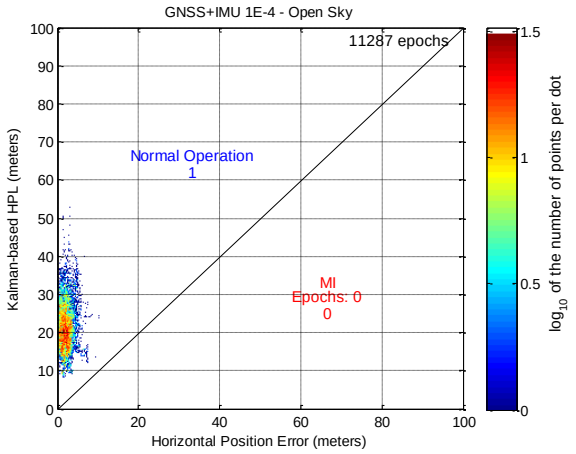

Figure 8 Madrid - Stanford diagram, GNSS+IMU, Open-Sky (TIR =1E-4)

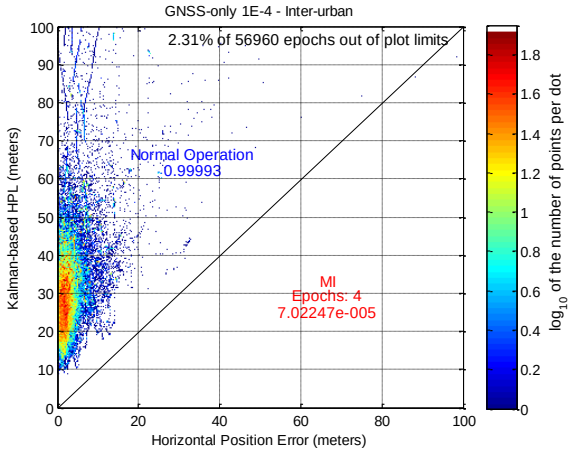

Figure 9 Madrid - Stanford diagram, GNSS-only, Inter-urban (TIR =1E-4)

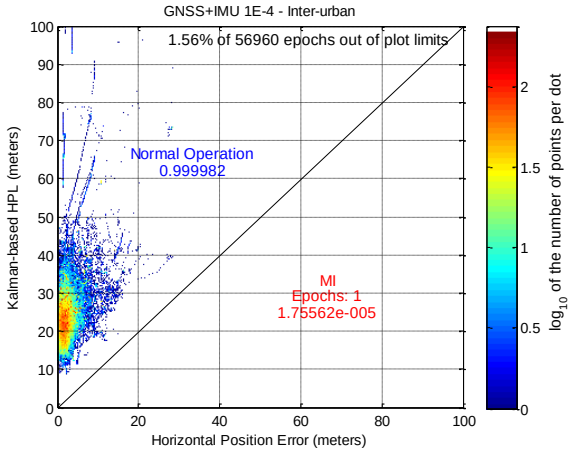

Figure 10 Madrid - Stanford diagram, GNSS+IMU, Inter-urban (TIR =1E-4)

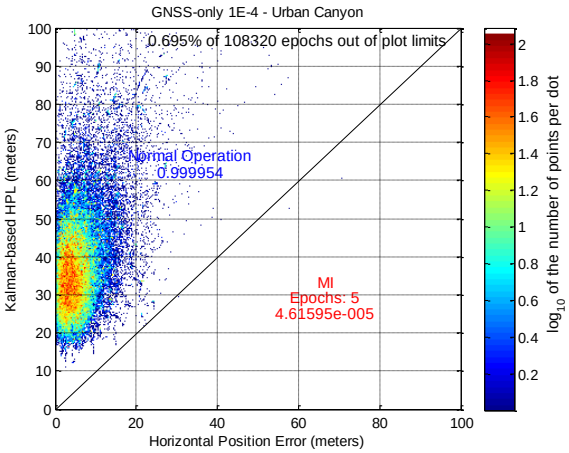

Figure 11 Madrid - Stanford diagram, GNSS-only, Urban (TIR =1E-4)

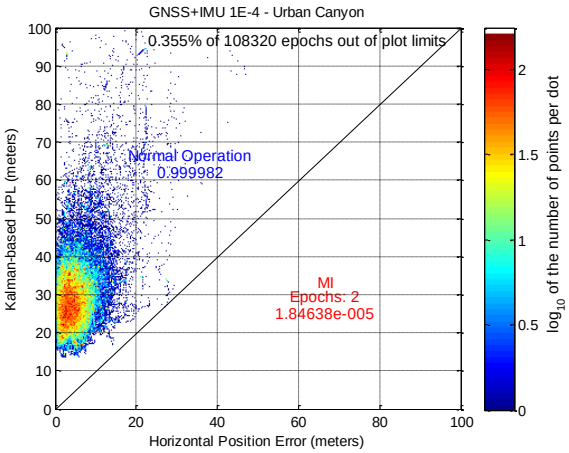

Figure 12 Madrid - Stanford diagram, GNSS+IMU, Urban (TIR =1E-4)

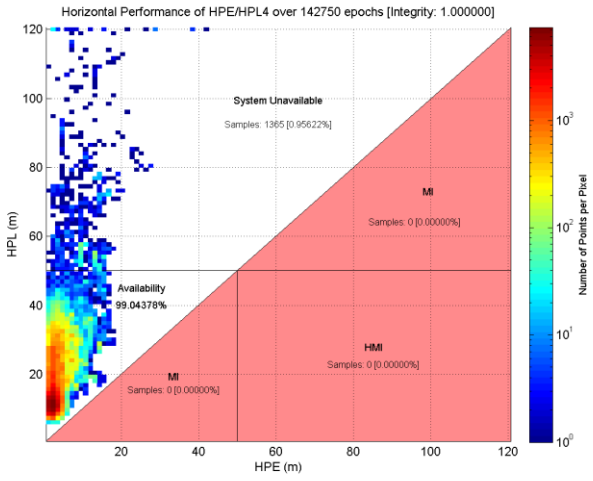

Figure 13 London - Stanford diagram, GNSS-only, Motorway (TIR=1E-4)

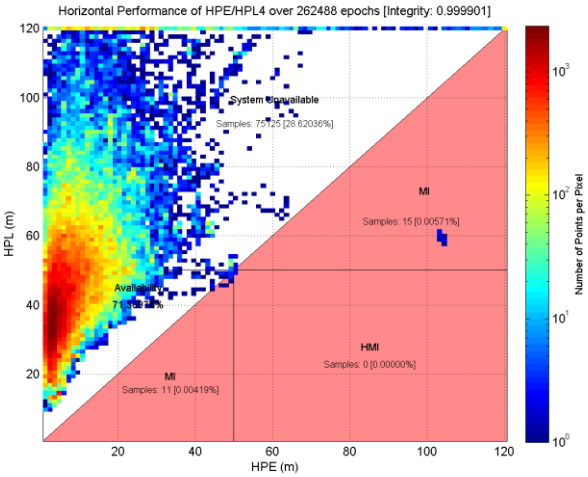

Figure 14 London - Stanford diagram, GNSS-only, Urban (TIR=1E-4)

PPP + KIPL

Precise Point Positioning (PPP) is a consolidated high precision positioning technique able to provide a position with a centimetre-level error. It is characterized by processing pseudorange and carrier-phase measurements, using accurate physical models and precise GNSS orbit & clock products. The PPP algorithm developed by GMV, *magicPPP*, provides a solution for both dual-frequency and single-frequency receivers. Moreover, *magicPPP* can be applied to both post-processing and real-time applications (which is the case of the ESCAPE project), provided that real-time input orbit and clock data (more concretely, orbit and clock corrections) are available.

As aforementioned, we have been working in developing an integrity layer to be added to the PPP positioning solution, necessary for the provision of certain critical application (such as Autonomous Driving), working with either dual or single frequency receiver.

During the last years, the evolution of the KIPL and PPP has been presented. The last results presented in [5] showed the performance of the KIPL+PPP in 6 test cases, including convergence tests and both static and kinematic scenarios for geodetic and low-cost receivers. In the case of the static scenarios, extensive analyses were done in order to obtain a representative Stanford diagram.

The extensive static test was based on the processing of four months (may-august 2017) of data from the GAP4 station (geodetic receiver, Topcon NetG5, using GPS and GLONASS) located in the GMV premises. Table 4 below contains the experimental rate of integrity failures for six different integrity risk values, for horizontal and vertical errors. The table columns contain the experimental rate of integrity failures, compared to the target integrity risk (TIR). This metric is computed by taking, for each target integrity risk, the overall fraction of epochs where the error is above the PL and normalizing by the corresponding TIR.

Hence, the integrity algorithm complies with the TIR whenever the metric is equal to or below 1. Although the biggest values of TIR do not correspond to realistic integrity requirements, they appear here to show the capability of the integrity algorithm to provide valid bounds for a wide range of values, based on an appropriate estimation of the solution error distribution.

TIR	0.1	0.05	0.01	0.001	1e-04	1e-07
H	0.49	0.41	0.22	0.25	0.1	0
V	0.56	0.44	0.16	0	0	0

Table 4: Relative (normalised with respect to Integrity Risk) rate of integrity failures in static scenario for different Target Integrity Risks (TIR) values

For better illustrating these results, Figure 15 is presented. It shows the Stanford diagram obtained for TIR=1e-07. It can be observed that the PLs are typically between 0.4 and 1 m.

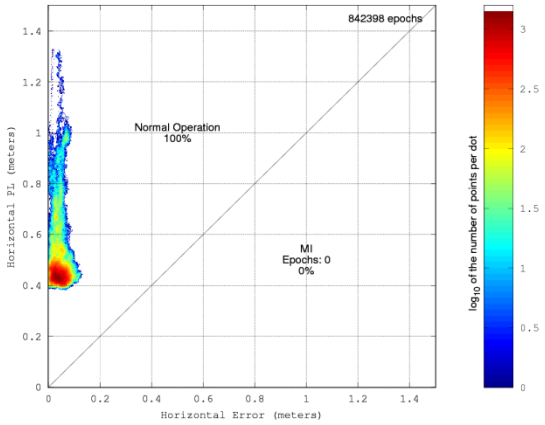

Figure 15 Stanford Diagram – Horizontal Component (TIR=1e-07)

As we can see, the integrity algorithm provides PL values of a few decimetres in this type of scenario, which are representative of open-sky conditions.

More information about this test, together with more tests analysing the behaviour of the KIPL under different conditions (from reconvergence periods to kinematic scenarios) can be found in [5].

PPP Improvements

During the past year, new improvements have been implemented in PPP. The most important improvements are: the multi-frequency processing and the hybrid GNSS/INS processing, using the IMU data in the PPP.

On the one hand, the multi-frequency processing allows to use all the available information coming from the satellites. The multi-frequency approach implemented by GMV combines observations from any number of individual frequencies and any number of ionosphere-free combination of these frequencies. In such a way, the observations of ionosphere-free combination allow a better estimation of positions and orbits, while the inclusion of observations from individual frequencies allows to estimate the ionospheric delay and to reduce the noise of the solution. The increase in the amount of information expectedly leads to an improvement in the quality of the estimated parameters. This is clearer for the case of Galileo frequencies, as increase of information related to the usage of E1, E5 and E5b is very large [11].

On the other hand, the inclusion of the IMUs has been included in the PPP algorithm. With this, a better performance of the PPP can be obtained in general, and especially when the receiver is in a harsh environment (e.g. deep urban canyon). Moreover, the KIPL has been improved to bound the solutions computed between GNSS updates by propagating with IMU data.

The approach followed is to process the IMU measurements in the propagation step within the Kalman filter already implemented in the PPP. Thus, while a solution using the GNSS measurements is given when the update of the Kalman filter is done, a solution (at a higher rate) is given during the propagation using IMU data.

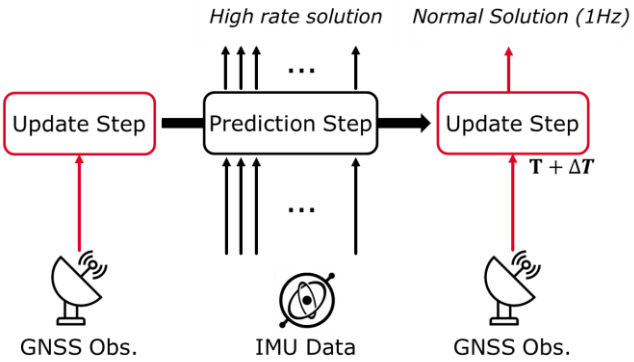

Figure 16 IMU Processing

As it can be seen in Figure 16, the IMU produces data at a rate higher than the GNSS receiver. With this, the output rate when using IMU data is higher than the one obtained only when using GNSS receiver data. Thus, a higher output rate of the KIPL is required in order to have a set of PLs given for each position computed. The main objective is to obtain a position and their associated PLs with a rate of around 10 Hz (one solution each millisecond).

The same scenario as in the previous section, located around Madrid has been used to have an estimation of the results that can be obtained with the PPP+KIPL when using both GNSS and IMU measurements.

First of all, we analyse the accuracy improvements obtained when using IMU measurements. The Root Mean Square (RMS) of the horizontal and vertical errors have been computed using only GNSS and using GNSS+IMU. Table 5 summarizes the obtained results:

	RMS Horizontal Error (m)	RMS Vertical Error (m)
GNSS-Only	3.4	5.8
GNSS+IMU	2.9	4.1
Improvement	**~14%**	**~30%**

Table 5: Accuracy improvements in PPP when using IMU data

As we can see in the previous table, an important improvement of the accuracy is obtained when IMU data is processed. Taking into account that this is a really hard scenario since it contains urban canyons (where not only the multipath effects are very important but also the reduced number of satellites in view and cycle-slips), a reduction of around a meter in the RMS of the positioning error is an important improvement.

Another important enhancement achieved when using IMU is the output rate. As aforementioned, a higher output rate is achieved when using IMU data (since the IMU produces data at a rate higher than the GNSS receiver). Thus, an output can be obtained with a rate higher than 1Hz.

Taking into account a part of the test (shown in Figure 17), the solutions obtained by the PPP when using GNSS-Only and when using GNSS+IMU are compared.

As we can see in Figure 17, while PPP solution obtained when using GNSS-Only is given each second (when GNSS measurements are available), PPP solution obtained when IMU data is processed has more rate.

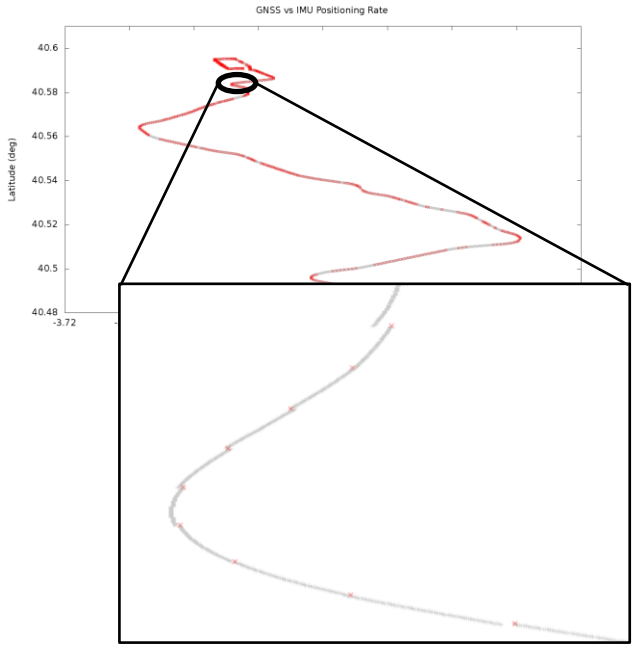

Figure 17 Trajectory computed using and not using IMU data (longitude (deg) vs. latitude (deg); solution obtained using GNSS-Only in red and solution obtained when using GNSS+IMU in grey)

In Figure 18, PLs (obtained using GNSS-only and GNSS+IMU) vs time have been plotted for a Target Integrity Risk of 0.05. It can be seen that there are points in grey (solution given by each propagation step of the Kalman filter using IMU data) between two red points (solution given by the update step of the Kalman filter using GNSS measurements). Moreover, it can be seen that the PL decreases in the case of the PPP using IMU measurements. Since the IMU measurements are better characterized, a better PPP performance is expected (see Table 5). It is shown in the reduction of the PLs when using GNSS+IMU.

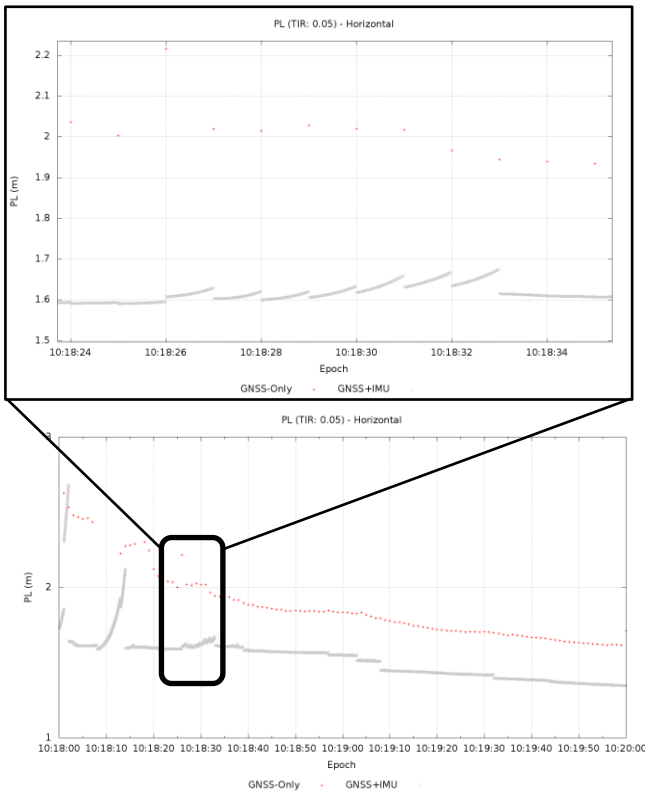

Figure 18 PL for TIR=0.05 using and not using IMU data (PL (m) vs. time; solution obtained using GNSS-Only in red and solution obtained when using GNSS+IMU in grey)

Finally, if a Stanford diagram is plotted for the horizontal error and PL obtained for TIR of 1E-07, the following figure is obtained:

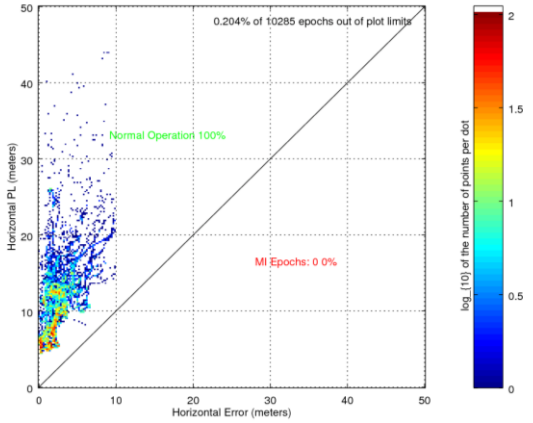

Figure 19 Stanford Diagram (TIR=1e-07) for GNSS+IMU

As we can see in Figure 19, the Target Integrity Risk is accomplished. This means that in the 100% of the epochs, the position error is smaller than the PL given with an integrity risk of 1E-07.

CONCLUSIONS

The paper has displayed the results obtained in **extensive field campaigns** with the GMV GNSS navigation and integrity technologies showing the results achieved in different conditions, from open-sky to harsh urban environments, by the Standard Hybrid GNSS/INS and PPP+IMU navigation algorithms.

The results show the **benefits of coupling the GNSS measurements with INS**, which improves the accuracy and considerably reduces the size of the PLs and the **high level of accuracy** achieved by the navigation algorithms:

- [Motorway]
  - Standard Hybrid GNSS/INS: <5m 95%
  - PPP+IMU: < 30 cm 95%
- [Urban]
  - Standard Hybrid GNSS/INS: <12m 95%
  - PPP+IMU: < 7m 95%

The KIPL integrity method has been tested in an extensive campaign:

- in different conditions: open-sky/motorway, inter-urban and urban environments
- with data from different types of GNSS receivers including low cost receivers
- with different Kalman filters: PPP and Hybrid Kalman filter (with and without inertial sensor measurements)

Thus proving that the KIPL is a reliability bound computation algorithm that offers integrity to any Kalman navigation solution:

- The obtained reliability bounds provide integrity failures percentages in the required intervals for different confidence levels in the analysed scenarios.
- The size of the bounds is consistent with the accuracy figures, and it seems difficult to define much smaller PLs that could guarantee integrity.

Therefore, the **KIPL integrity method** is a very good candidate to offer integrity to Kalman Filter based navigation systems, making it suitable for a wide range of applications requiring a reliable navigation solution like safety-critical applications (e.g. **Autonomous Driving**).

On the whole, the paper provides the accuracy, availability and integrity performances that can be achieved by GMV navigation technologies with different navigation algorithms and in different environments. The presented results show the benefits of hybridizing with other sensors like INS and the capabilities of the KIPL integrity method. These performances and considerations are an essential input in the design of automotive applications like autonomous driving in ESCAPE project ([1]), where the GMV GNSS navigation and integrity technologies will be combined with vehicle sensors and camera measurements to provide an accurate and reliable navigation solution.

REFERENCES

[1] ESCAPE (European Safety Critical Applications Positioning Engine) Project Website: http://www.gnss-escape.eu/

[2] Miguel Azaola et al., Isotropy-Based Protection Levels: a Novel Method for Autonomous Protection Level Computation with Minimum Assumptions, NAVITEC 2008, Noordwijk (The Netherlands), Dec 2008.

[3] Miguel Azaola and Joaquín Cosmen, Autonomous Integrity: An Error Isotropy–Based Approach for Multiple Fault Conditions, InsideGNSS, Jan-Feb 2009

[4] P. Navarro et al., Computing Meaningful Integrity Bounds of a Low-cost Kalman-filtered Navigation Solution in Urban Environments, ION GNSS+ 2015, Tampa, FL, USA.

[5] P. Navarro et al., PPP Integrity for Advanced Applications, Including Field Trials with Galileo, Geodecit and Low-Cost Receivers and a Preliminary Safety Analysis, ION GNSS+ 2016, Portland, Oregon, USA.

[6] Method for Autonomous Determination of Protection Levels for GNSS Positioning Based on Navigation Residuals and an Isotropic Confidence Ratio, Patent: Europe: EP2113786 (B1), USA: US8203482 (B2).

[7] Method for computing an error bound of a Kalman filter based GNSS position solution, Pending Patent: Europe EP14189240.6.

[8] srx-10 SW Defined Multi-Constellation GNSS Receiver: http://www.gmv.com/en/space/products/srx-10

[9] E. Domínguez et al., "Vehicular and Pedestrian GNSS Integrity Algorithms and Results for Urban and Road Environments Developed After an Extensive Real Data Collection Campaign," Proceedings of the 28th International Technical Meeting of The Satellite Division of the ION GNSS+ 2015, Tampa, Florida, September 2015, pp. 553-568.

[10] SRX-TRITON Multi-Antenna Front-End: http://www.gmv.com/en/space/products/srx-10/Front-end/

[11] P. Roldán et al., POD and PPP Multi-Frequency Processing, EGU General Assembly 2017, , Vienna, Austria.

[12] *magicPPP* webpage: https://www.gmv.com/en/Products/magicPPP/